PERFORMANCE ASSESSMENT OF MAXIMUM LIKELIHOOD IN THE DETECTION OF CARRIER INTERFERENCE CORRUPTED GPS DATA IN MOBILE HANDSETS

Taher AlSharabati

Electronics and Communications Engineering Department, Al-Ahliyya Amman University, Jordan

ABSTRACT

Mobile handset carriers are presented as a source of interference to GPS operation in smartphones. The carriers are presented in terms of their analytical form; block level generation as well as their statistical distribution model. In addition, we present the analytical form of the received GPS signal corrupted by carrier interference The Analysis is applied on the chip level in the acquisition engine before stripping the code or carrier. This expansion will restore the operation of GPS receiver in the presence of carrier interference. We present an estimate of the amount of improvement that Maximum Likelihood estimation gives in mitigating carrier interference in smartphones. The amount of improvement is compared to that of calculations based on measured data processing. The power spectral density of the interference is treated thoroughly to derive expressions for half of the noise power spectral density.

KEYWORDS

Detection, Average Carrier Power, Carrier Interference, Error Rate, Position Accuracy.

1. INTRODUCTION

Maximum Likelihood decoding (ML) is used in many receivers to reach at a "best guess" decision at what was actually transmitted from the transmitter in the presence of jammers. ML decoding requires some statistical parameters knowledge of the received signal and jammer. ML develops a statistical relation between all the possible transmitted symbols. In the example where the possible transmitted symbols are two, the one that has the highest weight is decided to be the transmitted symbol. ML decoding theory is treated in numerous resources. The intent here is to assess its performance.

The different services compacted in Smartphone are increasing. Those services have to co-exist with each other within a small proximity. However, with this co-existence there comes the price of affecting the performance of each other in the form of interference. Those effects are paramount when those services operate at the radio frequency (RF), especially, when those services are on the receiving end in the Smartphone, such as the GPS receiver. With GPS, there exist over the air (OTA) interface carrier technologies such as GSM, WCDMA and OFDM. These carriers transmit at a high power level (as high as 33dBm) as compared to the very low received GPS signal power (as low as -160dBm in some operating conditions). Hence, the GPS performance degrades most from OTA carrier inside a Smartphone.

DOI: 10.5121/ijcnc.2017.9304

Due to the non-ideal characteristics of the filter, part of the transmitter energy is encroached into adjacent bands. The non-ideal characteristics come from the non-ideal filter spectrum characteristics where spectrum response is not a brick wall performance (Figure 1). In many cases the power spectrum of the typical filter would present what is called "fly back" where filtering ceases to give adequate attenuation at higher/lower frequencies, which is a less stop band rejection performance in neighboring bands than the frequencies at the beginning of the stop band. This situation creates transmitter band noise into other bands (TX band noise). Power amplifier (PA) module (which includes a power amplifier and a filter) vendors tabulate PA performance based on which the band the noise encroaches upon. It should be mentioned that this is considered to GPS as unavoidable in-band interference. There is nothing that can be done to avoid it inside the phone. It can only be mitigated. It should be mentioned, however, that the spectral characteristics in Figure 1 are typical across-the-board of module manufacturers. They present the mere idea of spurious emissions into other bands (Figure 1) and typical numbers based on each transmit band. This is indeed problematic particularly to the mobile handset when the transmitter and receiver are within a very close proximity to one another to the point that there is not enough isolation between them. In fact, typical isolation figures (in dB) could be as high as a few dBs.

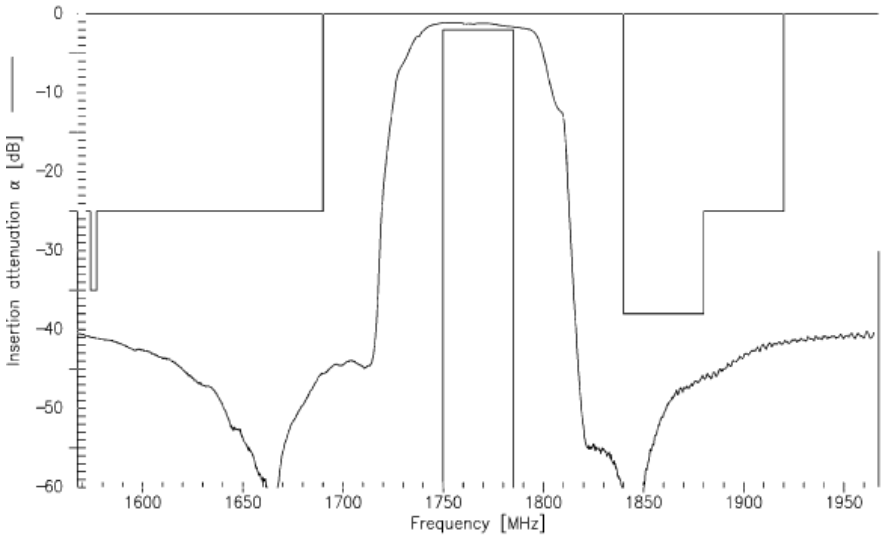

Figure 1 Typical Filter Power Spectrum Characteristics Showing "Fly-Back" [1]

2. ANALYSIS

In the following sections, we present modelling and derivation of the interference variance, the received signal, and the detection algorithm. Analysis of the interference is carried out on the baseband level by presenting the statistical models of the carriers' modulation schemes. The statistical variance of interference is derived. The complete model of the received signal is displayed.

2.1. The Variance of the Carrier Interference

The variance, σ^2, for the GSM case is

$$\boldsymbol{var}\left(\boldsymbol{v_{3G}(t)}\right)_{\boldsymbol{GSM}} = \boldsymbol{E}\left[\left(\boldsymbol{v_{3G}(t)}\right)_{\boldsymbol{GSM}}^{\boldsymbol{2}}\right]$$
$$= \boldsymbol{E}\left\{\left[\boldsymbol{V_{rms}}\left\{\boldsymbol{d_I(t)cos}\left(\frac{\boldsymbol{\pi t}}{\boldsymbol{2T}}\right)\boldsymbol{\cos(\omega_{IF}t)} + \boldsymbol{d_Q(t)\sin}\left(\frac{\boldsymbol{\pi t}}{\boldsymbol{2T}}\right)\boldsymbol{\sin(\omega_{IF}t)}\right\}\right]^{\boldsymbol{2}}\right\} \quad \textbf{(1)}$$

where E[ ] represents the expected value of the random process.

$$\boldsymbol{\sigma^2}_{\boldsymbol{GSM}} = \boldsymbol{V^2 rms^E}\left[\begin{array}{c} \boldsymbol{d_I^2(t)cos^2}\left(\boldsymbol{\omega_{IF}} + \frac{\boldsymbol{\pi}}{\boldsymbol{4}}\right) \\ \boldsymbol{+2d_I(t)d_Q(t)cos}\left(\frac{\boldsymbol{\pi t}}{\boldsymbol{2T}}\right)\boldsymbol{\sin}\left(\frac{\boldsymbol{\pi t}}{\boldsymbol{2T}}\right)\boldsymbol{\cos}\left(\boldsymbol{\omega_{IF}} + \frac{\boldsymbol{\pi}}{\boldsymbol{4}}\right)\boldsymbol{sin}\left(\boldsymbol{\omega_{IF}} + \frac{\boldsymbol{\pi}}{\boldsymbol{4}}\right) \\ \boldsymbol{+d_Q^2(t)sin^2}\left(\frac{\boldsymbol{\pi t}}{\boldsymbol{2T}}\right)\boldsymbol{sin^2}\left(\boldsymbol{\omega_{IF}} + \frac{\boldsymbol{\pi}}{\boldsymbol{4}}\right) \end{array}\right] \textbf{(2)}$$

The variance, σ^2, for the WCDMA case is

$$\boldsymbol{var}\left(\boldsymbol{v_{3G}(t)}\right)_{\boldsymbol{WCDMA}} = \boldsymbol{E}\left[\left\{\left(\boldsymbol{v_{3G}(t)}\right)_{\boldsymbol{WCDMA}}\right\}^{\boldsymbol{2}}\right]$$
$$= \boldsymbol{E}\left[\frac{\boldsymbol{V_{rms}}}{\sqrt{\boldsymbol{2}}}\left(\boldsymbol{d_I(t)cos}\left(\boldsymbol{\omega_{IF}t} + \frac{\boldsymbol{\pi}}{\boldsymbol{4}}\right) + \boldsymbol{d_Q(t)sin}\left(\boldsymbol{\omega_{IF}t} + \frac{\boldsymbol{\pi}}{\boldsymbol{4}}\right)\right)\right]^{\boldsymbol{2}} \quad \textbf{(3)}$$

Denote $var\left(v_{3G}(t)\right)_{WCDMA}$ as σ^2_{WCDMA}, then,

$$\boldsymbol{\sigma^2_{WCDMA}} = \frac{\boldsymbol{V_{rms}^2}}{\boldsymbol{2}}\boldsymbol{E}\left[\begin{array}{c} \boldsymbol{d_I^2(t)cos^2}\left(\boldsymbol{\omega_{IF}} + \frac{\boldsymbol{\pi}}{\boldsymbol{4}}\right) \\ \boldsymbol{+2d_I(t)d_Q(t)cos}\left(\boldsymbol{\omega_{IF}} + \frac{\boldsymbol{\pi}}{\boldsymbol{4}}\right)\boldsymbol{sin}\left(\boldsymbol{\omega_{IF}} + \frac{\boldsymbol{\pi}}{\boldsymbol{4}}\right) \\ \boldsymbol{+ d_Q^2(t)sin^2}\left(\boldsymbol{\omega_{IF}} + \frac{\boldsymbol{\pi}}{\boldsymbol{4}}\right) \end{array}\right] \quad \textbf{(4)}$$

The variance of the carrier interference, σ^2, is related to the noise power spectral density (PSD); N_0 through $\frac{N_0}{2}$. From Appendix A, the N_o for the WCDMA case:

$$\therefore \boldsymbol{N_{oWCDMA}} = \frac{\boldsymbol{V^2 rms}}{\boldsymbol{4}}\{(\boldsymbol{1 - sin2\omega_{IF}}) + (\boldsymbol{1 - cos2\omega_{IF}})\} \quad \textbf{(5)}$$

Likewise, for the GSM carrier (also from Appendix A):

$$\boldsymbol{N_{oGSM}} = \frac{\boldsymbol{V^2 rms}}{\boldsymbol{2}}(\boldsymbol{1 - cos}\frac{\boldsymbol{\pi t}}{\boldsymbol{T}}\boldsymbol{sin2\omega_{IF}}) \quad \textbf{(6)}$$

2.2. The Received Signal $r(n)$

The noise and GPS data are added together to form the GPS plus interference signal. According to the above numbers, $\omega_{IF} = 2\pi(9.548MHz)$, $T_s \cong 0.262ns$ and n would be large designating the sample number related to how many milliseconds of noise needed to be sampled and added to the GPS data. The addition operation of the samples of the noise to the samples of the GPS data occurs at the output of the ADC of the hardware platform collected in reference [2]. Then noise generated from the above procedure is added to the GPS data measured in [2]. In the discrete time domain;

$$r(n)_{WCDMA} = \overbrace{C^k(n)D^k(n)cos(\omega_{IF}n)}^{v^k_{GPS(n)}} + \underbrace{\frac{V_{rms}}{\sqrt{2}}\begin{Bmatrix} d_I(n)cos\left(\omega_{IF}nT_S + \frac{\pi}{4}\right) \\ +d_Q(n)sin\left(\omega_{IF}nT_S + \frac{\pi}{4}\right)\end{Bmatrix}}_{v_{3G(n)}} \quad (7)$$

$$r(n)_{GSM} = \overbrace{C^k(n)D^k(n)cos(\omega_{IF}n)}^{v^k_{GPS(n)}} + \underbrace{V_{rms}\begin{Bmatrix} d_I(nT_S)cos\left(\frac{\pi nT_S}{2T}\right)cos(\omega_{IF}nT_S) \\ +d_Q(nT_S)sin\left(\frac{\pi nT_S}{2T}\right)sin(\omega_{IF}nT_S)\end{Bmatrix}}_{v_{3G(n)}} \quad (8)$$

3. DESCRIPTION OF THE TEST SETUP AND RESULTS

3.1. General Model of the Setup

As shown in Figure 2, consider the transmitted signal (S_i) where it outputs M distinct messages. The received signal $r(n)$ is processed by the algorithm in [3] on the chip level in the Acquisition step. The detector, which is part of the Acquisition, tries to decide/estimate [4] which one of the S_i's was truly transmitted before it was corrupted by noise. The result is the estimated signal $\hat{S}_i$.

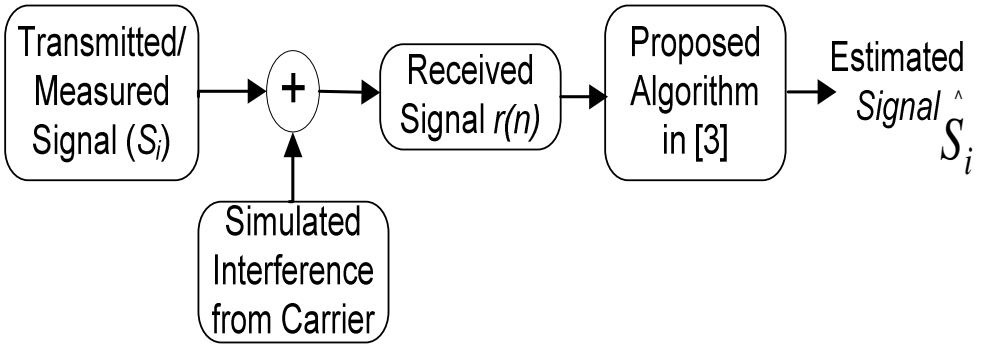

Figure 2 General Model of the Test Setup

The measured GPS data is readily available from the hardware in [2]. The carrier noise is generated on the simulation level and sampled at the sampling frequency of the hardware [2] used to collect the GPS data. This ensures that the noise is subjected to the same hardware specification as the measured GPS data. In addition, the noise link budget and power calculations were carried out according to the lineup gains, losses and specifications of the hardware lineup that was used to measure the GPS data. This establishes the controlled noise generation goes through the same the hardware as the measured GPS data. Both are then added as shown in Figure 2. Since the GPS data were measured using Software Defined Radio (SDR) platform, the acquisition engine was implemented using Matlab simulation software. Therefore, the methodology used to decrease the effect of the carrier noise was implemented in the simulation software embedded in the acquisition engine.

In order to obtain a user position, the GPS receiver must acquire and maintain a minimum of four satellites. The following results show, with the use of the scheme, the GPS receiver will maintain the minimum number of satellites to obtain the GPS fix while using the carrier service, which introduces the noise to the GPS receiver. Two data sets were used to test the methodology. These

two data sets were measured using two different SDR hardware platforms to insure applicability of the methodology across different platforms. The simulation parameters were changed according to each hardware platform lineup and architecture. One major difference between the two platforms is the sampling frequency, which was decreased from 38.192MHz in the first platform to 16.763MHs in the second platform.

The GPS data used in this paper is the data measured in [2], which is the data output of the ADC in an SDR platform. In Figure 3 below, eight satellites are shown to be detected by the GPS receiver along with their estimated Average Carrier Power (ACP) across the first four milliseconds of data collection. The ACP was calculated based [9] using

$$\boldsymbol{ACP = 10log(SNR) + 10log(BW) - 174dBm/Hz} \quad \textbf{(9)}$$

where SNR is the power of the satellite signal and BW is the bandwidth of integration. The threshold was determined using the standard deviation of the GPS data [5] collected in [2]. The threshold is a statistical quantity associated with the noise present above which a satellite signal peak is considered a true signal [5] and a satellite signal present. The standard deviation is that of noise since the received signal is below the noise floor and will not affect the statistics of the noise.

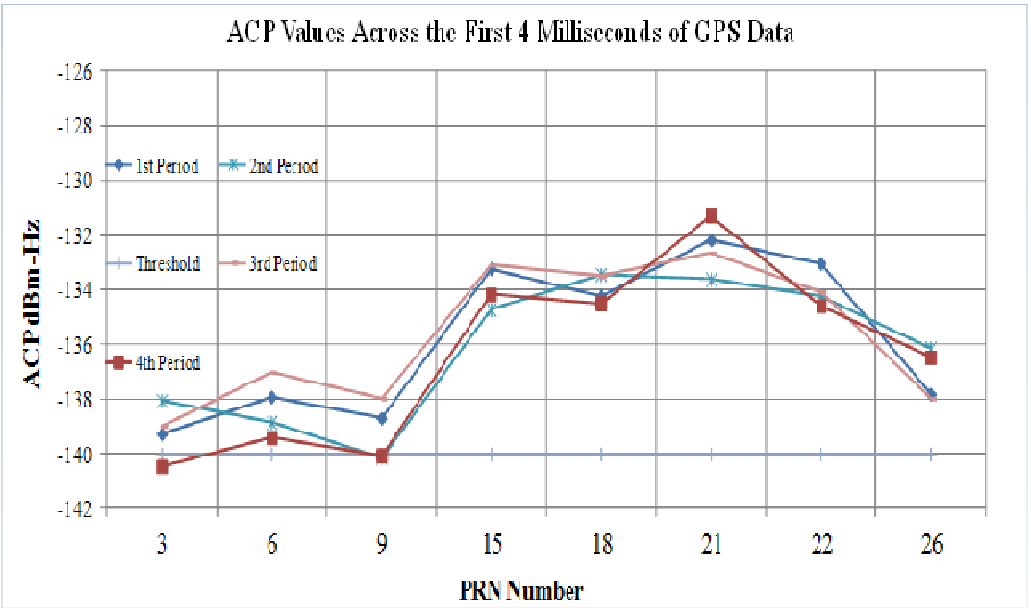

Figure 3 This figure shows the ACP changes with time, from one millisecond to the next, suggesting, while the data is considered a random process, and it is not stationary

The relationship between the SNR and chip energy to the noise PSD is via the ratio of chip rate to the bandwidth of the IF filter that controls the noise PSD:

$$\boldsymbol{SNR = \left(\frac{E_c}{N_0}\right)\left(\frac{R_c}{BW}\right)} \quad \textbf{(10)}$$

where R_c is the chip rate, $\frac{E_c}{N_0}$ is the chip energy to carrier noise power spectral density interference ratio, and BW is the bandwidth of the IF filter before the ADC.

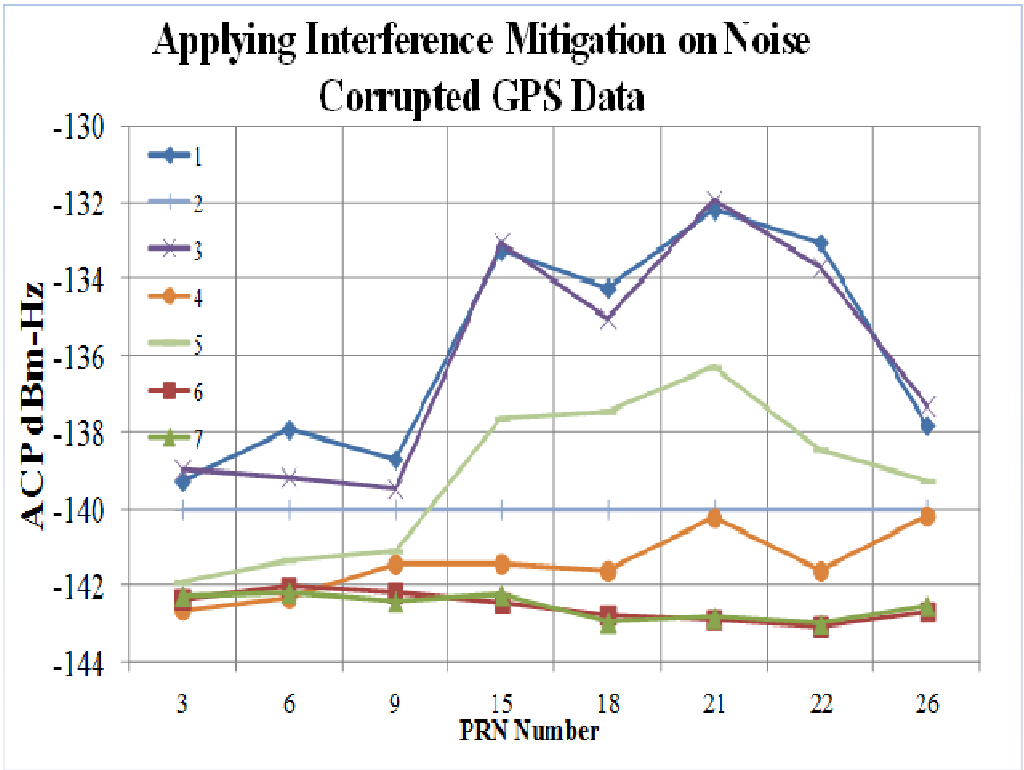

Figure 5 Applying Interference Mitigation on Noise Corrupted GPS Data-ACP vs. Satellite Number: (1) First Period before Adding Noise. (2) Threshold. (3) Algorithm Applied to GPS Data without Noise. (4) GPS Data after -155dBm/Hz of Noise Added. (5) GPS Data after -155dBm/Hz added and Algorithm used. (6) Noise Only Algorithm used. (7) Noise Only No Algorithm used.

Since the chips in CDMA of the GPS transmitted signal are BPSK modulated, the error rate is calculated based on the chip error rate (CER) equation for BPSK modulation: $CER = \frac{1}{2}erfc(\sqrt{Ec/No})$, $\frac{Ec}{No} = SNR(\frac{BW(2.046MHz)}{Rc(\frac{1.023Mc}{s})}$. Figure 7 also shows the amount of predicted improvement the algorithm provides in ACP between the cases when the algorithm used and when not used. Comparison between plot 2 and plot 3 gives that improvement prediction. Plot 2 shows the signal levels are low enough (below threshold) that result in an undetectable signal, before applying the algorithm to the corrupted GPS data.

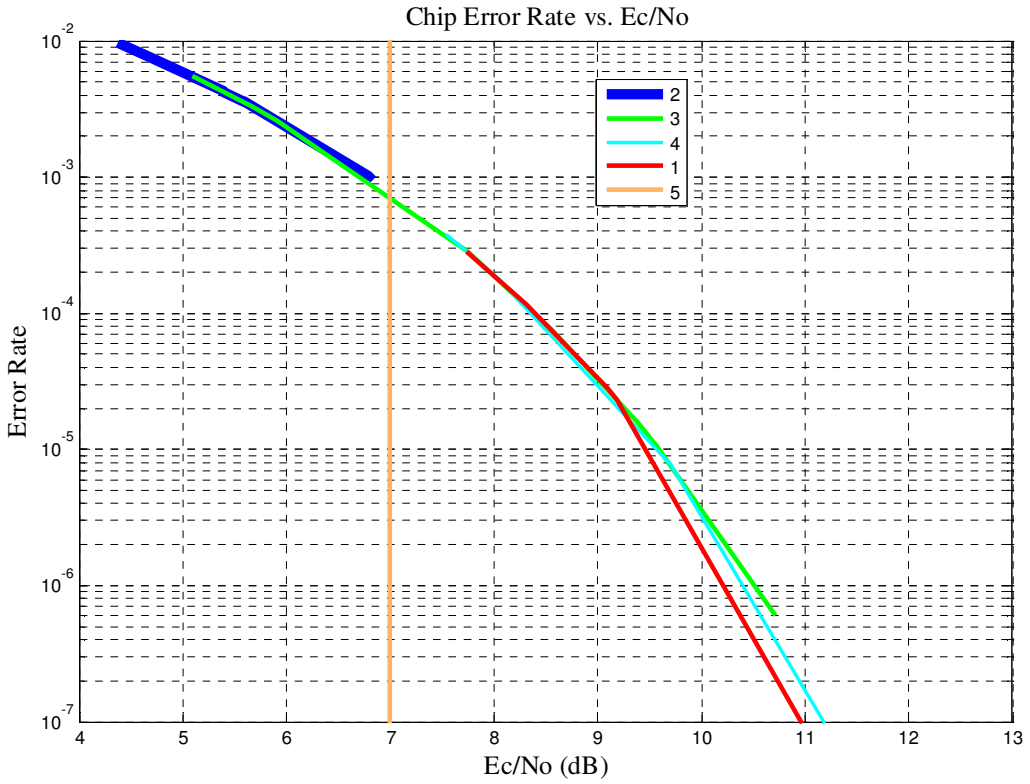

Figure 6 Applying Interference Mitigation to Noise Corrupted GPS Data-Error rate vs. E_c/N_o: (1) First Period before Adding Noise. (2) GPS Data Corrupted with -155dBm/Hz of Noise. (3) GPS Data Corrupted with -155dBm/Hz Noise and Algorithm Applied. (4) Algorithm Applied to GPS Data without Noise. (5) Threshold.

Table I Showing Scenarios under which the Algorithm Provides Improvement.

Noise Level dBm/Hz	Strongest ACP PRN	Average ACP PRN	Weakest ACP PRN
-155	B(1)	W(3)	NT(2)

(1) B: Satellite signal is being detected with both the algorithm and without the algorithm.
(2) NT: Satellite not tracked.
(3) W: Satellite signal is being detected with algorithm only.

While Table 1 shows under what conditions the algorithm provides improvements, it highlights if the algorithm provides the basic need for a GPS receiver to provide a user position or not. As stated above, the GPS receiver needs a minimum of four tracked PRNs to provide a GPS fix (user position). This critical information with its availability is provided in Figure 6 below, which shows the effect of applying the interference mitigation algorithm before and after introducing the carrier noise. Clearly, the algorithm does not affect the results when there is no noise introduced. Yet, after introducing the noise, significant improvements are obtained. These improvements are successfully maintaining a minimum of four satellites with adequate signal power, as compared to

the threshold, to be able to determine a user position. The improvements presented are in terms of increasing the ACP, which ultimately improve position accuracy and position fix. Figure 7 shows chip error rate vs. E_c/N_o. for five scenarios. It shows any signal with E_c/N_o to the right of the threshold; is considered a detectable signal; otherwise, it is not. Figure 7 can also be used as an estimate for the improvement of the algorithm proposed if the error rate is known. Then, this approach treats the performance of the algorithm as an assessment of the probability of error for ML decoding.

$\frac{E_c}{N_0}$ can also be estimated by approximating the performance of ML in Gaussian noise to that of OOK in non-coherent detection. Therefore,

$$\boldsymbol{Q\left(\frac{d}{2N_0}\right) = \frac{1}{2}e^{\frac{E_c}{2N_0}}} \quad \textbf{(11)}$$

where Q( ) is the complementary error function. Therefore,

$$\boldsymbol{\frac{E_c}{N_0} = 0.5\left(\frac{d}{2N_0}\right)^2} \quad \textbf{(12)}$$

where d is the difference between the means of the antipodal symbols of the received data Since $E[d_I(n)]$ and $E\left[d_Q(n)\right]$ in equations (18) and (19) are equal to zero, then

$$\boldsymbol{d = E\{[C^k(n)][D^k(n)]\cos(\omega_{IF}n) = 1\} - E\{[C^k(n)][D^k(n)]\cos(\omega_{IF}n) = -1\}} \quad \textbf{(13)}$$

Where

$E\{[C^k(n)][D^k(n)]\cos(\omega_{IF}n) = 1\}$ is the expected value of $[C^k(n)][D^k(n)]\cos(\omega_{IF}n)$ to equal "1"
and
$E\{[C^k(n)][D^k(n)]\cos(\omega_{IF}n) = -1\}$ is the expected value of $[C^k(n)][D^k(n)]\cos(\omega_{IF}n)$ to equal "-1". This estimate agreed with measured values with extreme correlation. The average carrier power of all the satellites from measured data was $C = -138.96dBm - Hz$ *while the estimate produced an average carrier power* $C = -139.448dBm - Hz$ *for a noise PSD level of -155dBm/Hz.*

3.1. Calculating Position Accuracy

One of GPS measurement accuracy parameters is the root mean squared (RMS) code tracking error in units of meters. Let us denote the RMS code tracking error as E then [6],

$$\boldsymbol{E = \sigma c} \quad \textbf{(14)}$$

where σ is the standard deviation in units of chips (noise variance) [7] and c is the speed of light. Each chip period is approximately 1μs. Figure 8 displays the RMS code tracking error (in meters) of the acquired satellites. It is evident, from this plot and that of Figure 6, that the extent that the average signal's power affects this parameter. The stronger the power is, the less the error is and therefore the more accurate the user position is. σ is calculated using a crude estimate [8] based on $\frac{C}{N_0}$ and the DLL loop bandwidth ($B_L = 2Hz$).

$$\sigma = T_c \frac{1}{\sqrt{SNR_L}} \quad (15)$$

$$SNR_L = \frac{C}{N_0} - 10\,log(B_L) \quad (16)$$

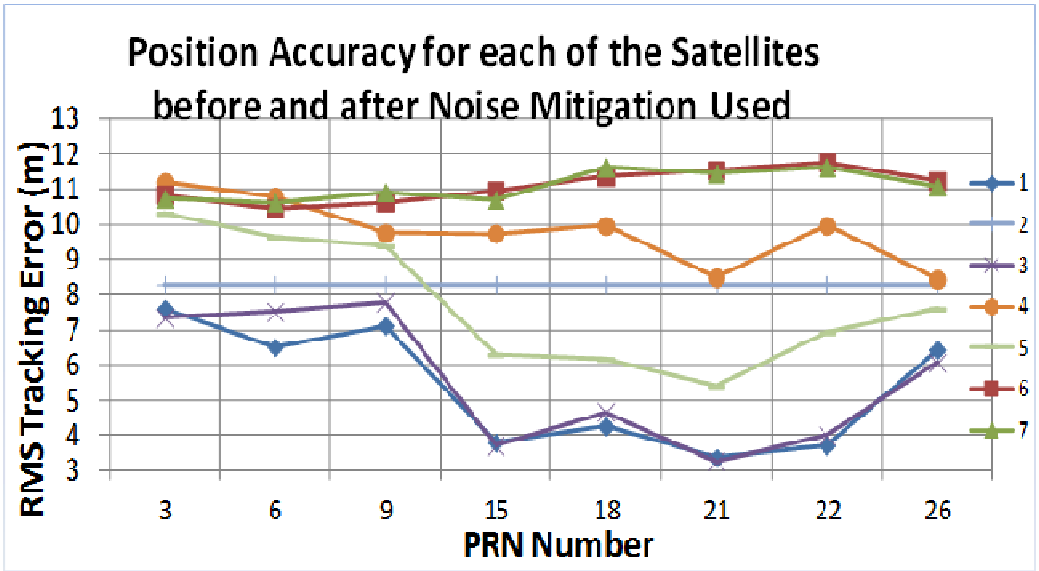

Figure 7 Position Accuracy for each of the Satellites before and after Noise Mitigation Used. (1) 1st Period before Adding Noise. (2) Threshold. (3) Algorithm Applied to GPS Data without Noise. (4) GPS Data after -155dBm/Hz of Noise Added. (5) GPS Data after -155dBm/Hz added and Algorithm used. (6) Noise Only Algorithm used. (7) Noise Only No Algorithm used.

4. CONCLUSION

In this paper, we demonstrated the statistical nature of the carrier interference, GPS data as well as the combined data stream of both. Their Gaussian distribution was clearly proved in terms of the analytical representations. The methodology, of treating the GPS data corrupted by noise to recover the satellites lost due to carrier noise, was systematically presented. In addition, it has a practical application and implementation inside the handset. Results show that the methodology can withstand high levels of noise power density while guaranteeing the minimum number of satellites to obtain a user position (a GPS fix).

5. APPENDIX A

5.1. The Variance of the Carrier Interference

Given that d_I and d_Q are zero mean random variables, their expected value, E[d_I] and E[d_Q] is zero. Also, since d_I and d_Q equal to ± 1, their squared value is "1" and therefore the expected value of their squared term, E[d_I^2] and E[d_Q^2], is "1". The variance, σ^2 for the WCDMA case, is

$$\frac{N_0}{2} = E\left[\left[\frac{V_{rms}}{\sqrt{2}}\left(d_I(t)cos\left(\omega_{IF}t + \frac{\pi}{4}\right) + d_Q(t)sin\left(\omega_{IF}t + \frac{\pi}{4}\right)\right)\right]^2\right] \quad \text{(A-1)}$$

$$\frac{N_0}{2} = \frac{V_{rms}^2}{2} E\begin{bmatrix} d_I^2(t)cos^2\left(\omega_{IF}+\frac{\pi}{4}\right) \\ +2d_I(t)d_Q(t)\cos\left(\omega_{IF}+\frac{\pi}{4}\right)\sin\left(\omega_{IF}+\frac{\pi}{4}\right) \\ +d_Q^2(t)sin^2\left(\omega_{IF}+\frac{\pi}{4}\right) \end{bmatrix} \quad \textbf{(A-2)}$$

$$d_I^2\frac{1}{2}\left(1+cos2\left(\frac{\pi}{4}+\omega_{IF}\right)\right) = \left[\frac{1}{2}\left(1+cos2\omega_{IF}cos\frac{\pi}{2}-sin\frac{\pi}{2}sin2\omega_{IF}\right)\right]$$
$$= \frac{1}{2}\left(1-sin2\omega_{IF}sin\frac{\pi}{2}\right) = \frac{1}{2}(1-sin2\omega_{IF}) \quad \textbf{(A-3)}$$

$$d_Q^2\frac{1}{2}\left(1-cos2\left(\frac{\pi}{4}+\omega_{IF}\right)\right) = \left[\frac{1}{2}\left(1-sin\frac{\pi}{2}cos2\omega_{IF}-sin2\omega_{IF}cos\frac{\pi}{2}\right)\right]$$
$$= \frac{1}{2}(1-cos2\omega_{IF}) \quad \textbf{(A-4)}$$

$$\therefore N_{o_{WCDMA}} = \frac{V^2rms}{4}\{(1-sin2\omega_{IF})+(1-cos2\omega_{IF})\} \quad \textbf{(A-5)}$$

Likewise, for the GSM carrier,

$$\frac{N_0}{2} = E\left\{\left[V_{rms}\left\{d_I(t)cos\left(\frac{\pi t}{2T}\right)\cos(\omega_{IF}t)+d_Q(t)sin\left(\frac{\pi t}{2T}\right)\sin(\omega_{IF}t)\right\}\right]^2\right\} \quad \textbf{(A-6)}$$

$$\frac{N_0}{2} = V_{rms}^2 E\begin{bmatrix} d_I^2(t)cos^2\left(\frac{\pi t}{2T}\right)cos^2\left(\omega_{IF}+\frac{\pi}{4}\right) \\ +2d_I(t)d_Q(t)cos\left(\frac{\pi t}{2T}\right)sin\left(\frac{\pi t}{2T}\right)cos\left(\omega_{IF}+\frac{\pi}{4}\right)sin\left(\omega_{IF}+\frac{\pi}{4}\right) \\ +d_Q^2(t)sin^2\left(\frac{\pi t}{2T}\right)sin^2\left(\omega_{IF}+\frac{\pi}{4}\right) \end{bmatrix} \quad \textbf{(A-7)}$$

$$d_I^2(t)cos^2\left(\frac{\pi t}{2T}\right)cos^2\left(\omega_{IF}+\frac{\pi}{4}\right) = \frac{d_I^2}{4}\left(1+cos\frac{\pi t}{T}\right)\left(1+cos2\left(\frac{\pi}{4}+\omega_{IF}\right)\right)$$
$$= \frac{1}{4}\left\{1+\underbrace{\cos\left(\frac{\pi}{2}+2\omega_{IF}\right)}_{-sin2\omega_{IF}}+cos\frac{\pi t}{T}+\underbrace{cos\frac{\pi t}{T}\cos\left(\frac{\pi}{2}+2\omega_{IF}\right)}_{-sin2\omega_{IF}cos\frac{\pi t}{T}}\right\} \quad \textbf{(A-8)}$$

$$\Rightarrow = \frac{1}{4}\left(1+cos\frac{\pi t}{T}\right)(1-sin2\omega_{IF}) \quad \textbf{(A-9)}$$

$$d_Q^2(t)sin^2\left(\frac{\pi t}{2T}\right)sin^2\left(\omega_{IF}+\frac{\pi}{4}\right) = \frac{d_Q^2}{4}\left(1-cos\frac{\pi t}{T}\right)\left(1-cos2\left(\frac{\pi}{4}+\omega_{IF}\right)\right)$$
$$= \frac{1}{4}\left\{1-\underbrace{\cos\left(\frac{\pi}{2}+2\omega_{IF}\right)}_{-sin2\omega_{IF}}-cos\frac{\pi t}{T}+\underbrace{cos\frac{\pi t}{T}\cos\left(\frac{\pi}{2}+2\omega_{IF}\right)}_{-sin2\omega_{IF}cos\frac{\pi t}{T}}\right\} \quad \textbf{(A-10)}$$

$$\Longrightarrow = \frac{1}{4}\left((1+sin2\omega_{IF})-cos\frac{\pi t}{T}(1+sin2\omega_{IF})\right) \quad \textbf{(A-11)}$$

$$= \frac{1}{4}(1 + sin2\omega_{IF})\left(1 - cos\frac{\pi t}{T}\right) \quad \textbf{(A-12)}$$

$$\therefore \quad N_{o_{GSM}} = \frac{V^2 rms}{4}\left[\left(1 + cos\frac{\pi t}{T}\right)(1 - sin2\omega_{IF}) + (1 + sin2\omega_{IF})\left(1 - cos\frac{\pi t}{T}\right)\right] = \frac{V^2 rms}{4}\left[1 - sin2\omega_{IF} + cos\frac{\pi t}{T} - cos\frac{\pi t}{T}sin2\omega_{IF} + 1 - cos\frac{\pi t}{T} + sin2\omega_{IF} - cos\frac{\pi t}{T}sin2\omega_{IF}\right] = \frac{V^2 rms}{2}\left(1 - cos\frac{\pi t}{T}sin2\omega_{IF}\right) \quad \textbf{(A-13)}$$

$$= \frac{V^2 rms}{2}\left(1 - cos\frac{\pi t}{T}sin2\omega_{IF}\right) \quad \textbf{(A-14)}$$

$$\therefore \quad N_{o_{GSM}} = \frac{V^2 rms}{2}\left(1 - cos\frac{\pi t}{T}sin2\omega_{IF}\right) \quad \textbf{(A-15)}$$

REFERENCES

[1] EPCOS. "SAW Components SAW Tx Filter KPCS & UMTS 1700." EPCOS B39182B9441M410. EPCOS, 23 July 2009. Web. 5 Feb. 2016. http://dtsheet.com/doc/564321/epcos-b39182b9441m410>.

[2] Borre, K., Akos, D. M., Bertelsen, N, Rinder, P, and Jensen, S. H., A Software Defined GPS and Galileo Receiver, Chapter 5, Birkhauser, 2007.

[3] AlSharabati, T., Chen, Y. "Statistical Approach to Mitigating 3G Interference to GPS in 3G Handset," International Journal of Communications,Network and System Sciences, Vol. 3, No. 9, September 2010, pp. 730-736.

[4] Barakat, M., Signal Detection and Estimation, 2nd Ed., Chapter 5, Artech House, 2005.

[5] Tsui, J. B., Fundamental of Global Positioning System. A Software Approach, 2nd Ed., Wiley, 2005.

[6] Betz, J. W., "Effect of Narrowband Interference on GPS Code Tracking Accuracy," ION NTM, 26-28 January 2000, pp. 16-27.

[7] Braasch, M. S. and Van Dierendonck, A. J., "GPS Receiver Architecture and Measurements," Proceedings of the IEEE, Vol. 87, No. 1, 1999, pp. 48-64.

[8] Bradford W. Parkinson; Per Enge; Penina Axelrad; James J. Spilker Jr., Global Positioning System: Theory and Applications, Volume I, American Institute of Aeronautics and Astronautics, 1996.

[9] SiRF Internal Document.

Authors

Taher AlSharabati obtained his BSEE from St. Cloud State University in 1993, his MSEE from the University of Toledo in 1996, and his PhD in Electrical Engineering from the University of South Carolina in 2012. Between his MSEE and PhD, he worked in the industry for many years during which he worked at Motorola Inc. for about nine years. Currently, he is an assistant professor at Al Ahliyya Amman University in the Electronics and Communications Engineering department.